Computational Study of Ring- and Metal-Protonated Ferrocene

Michael L. McKee

Contribution from the Department of Chemistry, Auburn University, Auburn, Alabama 36849

Received May 27, 1992

Abstract: Protonated ferrocene was studied at several different levels of theory. Geometries were optimized at the Hartree–Fock level with an effective core potential for iron and a 6-31G* basis for carbon and at the MP2 level of electron correlation with an all-electron basis. The largest basis set used included a 6-31G* basis on carbon and triple-ζ d-functions plus f-functions on iron. At the HF level, the ring-protonated site is favored over the metal-protonated site, but electron correlation at the MP2 level has a very large effect on the relative energy of the two structures and causes a reversal in the preferred site. While geometries found including electron correlation are considerably different from HF geometries, the preference for metal protonation is maintained. Interestingly, an entirely different mode of binding is predicted for ring protonation at the MP2 level of geometry optimization. Analysis of the charges and metal populations indicates that metal protonation causes nearly a full electron to be transferred from the rings to the metal. On the other hand, if the ring is protonated, the charge on iron does not substantially change.

Introduction

While the proton affinity of ferrocene is well established, the site of protonation is not. In solution and in the presence of a strong acid, an NMR study[1] has established that ferrocene is protonated on the metal and an IR study[2] has shown that the rings are bent away from the metal in solution. However, in less acidic solutions and in the gas phase, evidence has been presented favoring protonation on the metal, the cyclopentadienyl (Cp) ring, or an agostic position bridging the metal and the ring.[3-7]

In weakly protic solvents, such as chloroform, hydrogen bonding is found[8] to occur preferentially with the Cp ring of ferrocene, while, in strongly acidic media, metal protonation occurs. In another study,[9] it was determined that perfluoro-*tert*-butyl alcohol hydrogen bonded to the Cp ring in liquid Xe at 165–270 K.

Several groups have determined the proton affinity of ferrocene.[10] Foster and Beauchamp obtained[3] an early value of 213 ± 4.5 kcal/mol. From measurements of proton equilibria, Ikonomou, Sunner, and Kebarle found[4] values of 205.9 ± 1.5 kcal/mol for the proton affinity and 7.2 ± 2.0 cal/(K·mol) for the entropy change. Also from equilibrium measurements, Meot-Ner determined[5] values of 207 ± 1 kcal/mol and 6.3 ± 1 cal/(K·mol) for the proton affinity and entropy change, respectively. The increase in entropy that results from protonation can be largely attributed to a reduction of the symmetry factor.[4,5] However, the entropy change does not give information on the site of protonation.

A pulsed-ionization high-pressure mass spectrometric study by Allison et al.[6a] supported protonation on the metal for $Fe(CO)_5$ but on the ring or an 'agostically bonded position bridging the ring and the metal' for $FeCp_2$. When CID spectra were taken of both protonated complexes, no H-containing neutral fragments were found for $HFe(CO)_5^+$ while a C_5H_6 fragment was frequently lost from protonated ferrocene.

Two groups have estimated the energy difference between protonation on the metal and on the ring. Meot-Ner estimated[5] the ring site was at least 5 kcal/mol less favorable from a deuterium labeling experiment. Ikonomou, Sunner, and Kebarle speculated[4] that the free energy of the ring site might be about 10 kcal/mol less favorable than that of the metal site. They observed a curved Arrhenius plot for the proton exchange between ferrocene and acetophenone which might indicate that a second reaction channel (i.e. ring protonation) becomes competitive at intermediate temperatures.

The site of protonation has direct relevance on the mechanism of Friedel–Crafts acylation of ferrocene, a well-known and widely used reaction. The standard mechanism[11] indicates the formation of an initial complex between an electrophile and the metal followed by endo attack of the electrophile on the ring. Ring substitution occurs following loss of a proton from the exo face of the ring. Recently, Cunningham[7] has summarized evidence favoring initial exo attack and reports the "first unequivocal examples of intermolecular Friedel–Crafts acylation of ferrocene derivates occurring by exo attack of the electrophile". He also suggests that protonation of ferrocenes could occur by exo attack on the ring rather than direct protonation of the metal.

Theoretical calculations may make a valuable contribution to resolving this question. However, ferrocene has been slow to succumb to the advance of theoretical methods. Its reputation as the "enfant terrible"[12] of transition metal complexes is justly deserved. Almlöf and co-workers[13,14] have spent considerable effort determining the computational level required to obtain an accurate metal–ring distance. At the Hartree–Fock level using relatively good basis sets, the iron–ring distance is calculated to

(1) Curphey, T. J.; Santer, J. O.; Rosenblum, M.; Richards, J. H. *J. Am. Chem. Soc.* **1960**, *82*, 5249.
(2) Pavlik, I. J. *Collect. Czech. Chem. Commun.* **1967**, *32*, 76.
(3) Fosier, M. S.; Beauchamp, J. L. *J. Am. Chem. Soc.* **1975**, *97*, 4814.
(4) Ikonomou, M. G.; Sunner, J.; Kebarle, P. *J. Phys. Chem.* **1988**, *92*, 6308.
(5) Meot-Ner (Mautner), M. *J. Am. Chem. Soc.* **1989**, *111*, 2830.
(6) (a) Allison, C. E.; Cramer, J. A.; Hop, C. E. C. A.; Szulejko, J. E.; McMahon, T. B. *J. Am. Chem. Soc.* **1991**, *113*, 4469. (b) Hop, C. E. C. A.; McMahon, T. B. Private communication.
(7) Cunningham, A. F., Jr. *J. Am. Chem. Soc.* **1991**, *113*, 4864.
(8) Cerichelli, G.; Illuminati, G.; Ortaggi, G. *J. Organomet. Chem.* **1977**, *127*, 357.
(9) Lokshin, B. V.; Kazarian, S. G.; Ginzburg, A. G. *J. Mol. Struct.* **1988**, *174*, 29.
(10) Martinho Simões, J. A.; Beauchamp, J. L. *Chem. Rev.* **1990**, *90*, 629.
(11) (a) Purcell, K. F.; Kotz, J. C. *Inorganic Chemistry*; Saunders: Philadelphia, PA, 1977; p 925. (b) Cotton, F. A.; Wilkinson, G. *Advanced Inorganic Chemistry*, 5th ed.; Wiley: New York, 1988; p 1176. The authors also note that "it seems more likely that the electrophile attacks the ring in the exo position with the endo H then moving to the metal and being subsequently lost".
(12) (a) Jungwirth, P.; Siussi, D.; Weber, J. *Chem. Phys. Lett.* **1992**, *190*, 29. (b) See also: Cook, D. B. *Int. J. Quantum Chem.* **1992**, *43*, 197.
(13) (a) Lüthi, H. P.; Ammeter, J. H.; Almlöf, J.; Faegri, K. *J. Chem. Phys.* **1982**, *77*, 2002. (b) Almlöf, J.; Faegri, K.; Schilling, B. R.; Lüthi, H. P. *Chem. Phys. Lett.* **1984**, *106*, 266. (c) Lüthi, H. P.; Siegbahn, P. E. M.; Almlöf, J.; Faegri, K.; Heiberg, A. *Chem. Phys. Lett.* **1984**, *111*, 1.
(14) Park, C.; Almlöf, J. *J. Chem. Phys.* **1991**, *95*, 1829.

0002-7863/93/1515-2818$04.00/0

be much longer than experiment[15] (Table I; R_{calc} = 1.88–1.90 Å; R_{exptl} = 1.66 Å). If the MP2 method is used with moderate basis sets, the Fe–ring distance is calculated too short (1.58–1.59 Å). This was attributed to the absence of single excitations in the MP2 method, since the MCPF method,[16] which accounts for single excitations, yielded a more reasonable metal–ring distance.[14] When single excitations are excluded from the MCPF calculation, the metal–ring distance increased almost 0.1 Å.[14] Almost quantitative agreement is found if all 66 valence electrons are correlated in the MCPF treatment and a correction is made for ligand–ligand dispersion.[14]

On the other hand, density functional theory (DFT) shows promise for the study of transition metals.[17] The calculated Fe–ring distance is 1.585 Å when the local-density approximation is used and increases to 1.648 Å when corrections are made for nonlocal exchange and correlation.[17]

Two theoretical calculations have been reported for protonated ferrocene.[12a,18] In one, the extended Hückel method was used to predict a reactivity index to describe the favorable sites for electrophilic or nucleophilic addition.[18] The second contribution by the same group[12a] included calculations using the local spin density (LSD) method and the HF method. The interaction of a proton with ferrocene was calculated along the equatorial axis and along the 5-fold axis. After partial geometry optimization, metal protonation was preferred with a protonation energy of −201.3 kcal/mol using the LSD method and −158.5 kcal/mol using the HF method.

Method

Two theoretical studies[19,20] of iron–ligand bonding have found that a single configuration, properly chosen and corrected for electron correlation, can provide a qualitatively correct description of iron–ligand bonding. The first report[19] dealt with the interaction of Fe with simple ligands while the more recent one[20] dealt with the mechanism of ferrocene formation from iron atoms plus cyclopentadiene.

The method utilizes an effective core potential (ECP) as described by Hay and Wadt[21] for the 18 core electrons of iron and a double-ζ basis set for the valence shell of iron (3s2p5d → 2s2p2d). The double-ζ basis set of Dunning and Huzinaga was used for carbon and hydrogen.[22] The resulting basis set was referred to as ECPDZ (effective core potential; double-ζ).[19,20] This same basis set has been used by Morokuma and co-workers[23] in their study of catalytic cycles.

Veldkamp and Frenking[24] have found that improved iron–ligand bond energies are obtained if the effective core potential of iron is limited to only 10 electrons[25] (1s, 2s, and 2p electrons) and the valence orbitals are described with at least a double-ζ quality basis set. These authors also found that at least a valence double-ζ plus polarization basis set is required for carbon. For these reasons, the current study was carried out with the 10-electron HW-ECP[25] rather than the 18-electron HW-ECP[21] and the 6-31G* basis set was used for carbon and hydrogen. Recently, the 10-electron HW-ECP was included in a study[26] of several ECP methods which compared the splitting between low-lying states of Fe, ionization potentials, and electron affinities with experiment.

Table I. Comparison of Calculated Iron–Ring Distances (Å)

basis (Fe/C,H)	iron–ring	Fe–C	C–C	C–H
(5,4,3)/TZ[a]	1.894	2.256	1.440[b]	1.104[b]
(4,4,3,1)/DZ[a]	1.889	2.251	1.440[b]	1.104[b]
(4,4,3,1)/TZ[a]	1.912	2.271	1.440[b]	1.104[b]
MP2 (66 el)[a]	1.58	1.999	1.440[b]	1.104[b]
ECPDZ/DZ[c]	1.931	2.287	1.422	1.068
BAS2/6-31G*[d]	1.839	2.196	1.410	1.072
MP2/BAS1 (56 el)/6-31G*[d]	1.540	1.976	1.456	1.084
MP2/BAS1 (90 el)/6-31G*[d]	1.517	1.959	1.458	1.085
MCPF (66 el) + dispersion + BSSE correction[a]	1.677	2.077	1.440[b]	1.104[b]
LDA[e]	1.585	1.993	1.421	1.093
LDA/NL[e]	1.648	2.049	1.432	1.091
exptl[f]	1.65–1.66	2.05–2.06	1.440	1.104

[a] Reference 14. [b] Fixed. [c] Reference 20. [d] This work. [e] Reference 17. [f] Reference 15.

Table II. Descriptions of Basis Sets Used

	BAS1	BAS2	BAS3
Fe	533/53/5[a] → 5333/521/41 (23 functions/Fe)	core: 10-electron HW-ECP[b] valence: 55/5/5[b] → 441/41/41 (19 functions/Fe)	5333/53/5[a] → 53321/521/41 + diffuse d + f-functions (36 functions/Fe)
C,H	6-31G (110 functions/2Cp)	6-31G*[c] (160 functions/2Cp)	6-31G*[c] (160 functions/2Cp)

[a] Number of primitives in each contracted function for s/p/d orbitals. Huzinaga basis. [b] Reference 25. [c] The calculations used the set of 5d orbitals while the designated 6-31G* basis uses 6d orbitals.

While some cancellation of error is expected between ferrocene and protonated ferrocene, the different modes of bonding involved in the two protonation sites require a fairly good computational level. Since Veldkamp and Frenking[24] found little change in the iron–ligand bond energy beyond the MP2 level of electron correlation, calculations will be carried out only at the MP2 level which is very efficiently programmed in GAUSSIAN 92.[27] For computational convenience, the set of 5 d functions was used on carbon rather than the normal set of 6 d functions.

The original basis set describing the valence shell of Fe included two contracted s orbitals, one contracted p orbital, and one contracted d orbital, each made up of five primitive gaussians (i.e. (55/5/5)).[25] A more flexible basis set was constructed by independently varying the most diffuse primitive function to give a (441/41/41) basis set.[28] This basis set will be denoted BAS2 and was used for geometry optimization at the Hartree–Fock level.

Two basis sets were used for all-electron calculations, both based on the (5333/53/5) basis set for iron described by Huzinaga.[29] The smaller basis set (BAS1) was constructed from the (5333/53/5) basis set for iron by splitting off the most diffuse p and d shell, giving a (5333/521/41) basis. In addition, the 6-31G basis was used for carbon and hydrogen. The larger basis set (BAS3) was constructed by splitting off the most diffuse s, p, and d function, giving a (53321/521/41) basis set. An additional diffuse d function (exponent = 0.11) and a set of f functions (exponent = 3.0) were added giving a final basis set of (53321/521/411/1). The 6-31G* basis set was used for carbon and hydrogen. Details are summarized in Table II.

The BAS1 basis set was used for MP2 optimizations where the "frozen core" approximation was used for calculating the MP2 energy and gradients. Each cycle of optimization for the protonated forms required approximately 1 cpu hour on a Cray YMP, and the optimization was run for at least 25 cycles. After 25 cycles of optimization, the energy change on successive cycles was much less than 1 kcal/mol. Therefore, the

(15) Haaland, A. *Top. Curr. Chem.* **1975**, *53*, 1.
(16) Chong, D. P.; Langhoff, S. R. *J. Chem. Phys.* **1986**, *84*, 5606.
(17) Fan, L.; Ziegler, T. *J. Chem. Phys.* **1991**, *95*, 7401.
(18) Weber, J.; Fluekiger, P.; Stussi, D.; Morgantini, P.-Y. *THEOCHEM* **1991**, *227*, 175.
(19) McKee, M. L. *J. Am. Chem. Soc.* **1990**, *112*, 2601.
(20) McKee, M. L. *J. Phys. Chem.* **1992**, *96*, 1683.
(21) Hay, P. J.; Wadt, W. R. *J. Chem. Phys.* **1985**, *82*, 270.
(22) Dunning, T. H.; Hay, P. J. *Modern Theoretical Chemistry*; Plenum: New York, 1976; pp 1–28.
(23) (a) Obara, S.; Kitaura, K.; Morokuma, K. *J. Am. Chem. Soc.* **1984**, *106*, 7482. (b) Koga, N.; Obara, S.; Kitaura, K.; Morokuma, K. *J. Am. Chem. Soc.* **1985**, *107*, 7109. (c) Koga, N.; Morokuma, K. *J. Am. Chem. Soc.* **1986**, *108*, 6136. (d) Koga, N.; Jin, S.-Q.; Morokuma, K. *J. Am. Chem. Soc.* **1988**, *110*, 3417. (e) Nakamura, S.; Morokuma, K. *Organometallics* **1988**, *7*, 1904. (f) Daniel, C.; Koga, N.; Han, J.; Fu, X.-Y.; Morokuma, K. *J. Am. Chem. Soc.* **1988**, *110*, 3773. (g) Koga, N.; Morokuma, K. *J. Phys. Chem.* **1990**, *94*, 5454. (h) Koga, N.; Morokuma, K. *Organometallics* **1991**, *10*, 946.
(24) (a) Veldkamp, A.; Frenking, G. *J. Chem. Soc., Chem. Commun.* **1992**, 118. (b) Veldkamp, A.; Frenking, G. *J. Comput. Chem.* **1992**, *13*, 1184.
(25) Hay, P. J.; Wadt, W. R. *J. Chem. Phys.* **1985**, *82*, 299.
(26) Leininger, T.; Jeung, G.-H.; Rohmer, M.-M.; Pélissier, M. *Chem. Phys. Lett.* **1992**, *190*, 342.
(27) Frisch, M. J.; Trucks, G. W.; Head-Gordon, M.; Gill, P. M. W.; Wong, M. W.; Foresman, J. B.; Johnson, B. G.; Schlegel, H. B.; Robb, M. A.; Replogle, E. S.; Gomperts, R.; Andres, J. L.; Raghavachari, K.; Binkley, J. S.; Gonzalez, C.; Martin, R. L.; Fox, D. J.; DeFrees, D. J.; Baker, J.; Stewart, J. J. P.; Pople, J. A. Gaussian 92; Gaussian, Inc.: Pittsburgh, PA, 1992.
(28) The exponent of the most diffuse primitive s-gaussian is the same for both contracted s-functions. Since it is independently varied in one contracted set, it was deleted from the other contracted set (thus, 441/41/41 rather than 541/41/41).
(29) Huzinaga, S. *Gaussian Basis Sets for Molecular Calculations*; Elsevier: New York, 1984.

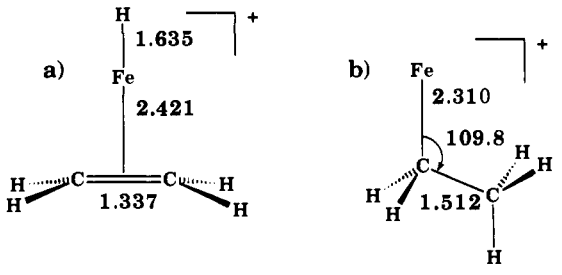

Figure 1. Selected geometric parameters are given at the UHF/BAS2 level for (a) HFe—H_2C=CH_2^+ and (b) Fe—$C_2H_5^+$. Both complexes are high spin.

optimization was halted even though the full internal stopping criterion was not reached.

The BAS1 basis set was also used to analyze the wave function using Bader's method of integrating over atomic basins.[30] The method avoids the arbitrary division of electron density between atomic centers and is found to be more independent of the level of calculation than other methods. Recent improvements[31] have been made to the program[32] which integrates electron densities, making the application of the method to molecules as large as ferrocene feasible. Cioslowski and Mixon[33] have recently reported a covalent bond order which is based on the integrated basins. These covalent bond orders do not rely on "atomic orbitals" and are largely independent of the basis set used.[34]

Results and Discussion

The eclipsed geometry of ferrocene was optimized in D_{5h} symmetry at the HF/BAS2 level. The HF/BAS2 Fe–C distance is in much better agreement with experiment than the HF/ECPDZ value,[20] but it is still overestimated by 0.14 Å compared to experiment (Table I). On the other hand, the Fe–C distance at the MP2/BAS1 level is too short, but by a smaller amount (0.07 Å). The "full core" MP2 approximation has the effect of decreasing the Fe–C distances by 0.02 Å compared to the "frozen core" MP2 calculations (Table I). The disagreement between the MP2 geometry obtained here and the MP2 geometry reported by Almlöf and co-workers[14] results because the bases for iron are different (4s3p2d versus 5s4p3d) and because the geometry reported in Table I was fully optimized while Almlöf and co-workers only optimized the iron-ring distance.

Since the iron-ring distance is calculated too long by the HF/BAS2 method, the binding energy of the Cp rings will be underestimated. This is clearly demonstrated by single-point calculations with the MP2/BAS3 method at the geometry obtained at the HF/BAS2 and MP2/BAS1 levels. The MP2/BAS3 energy at the correlated geometry is 41.2 kcal/mol lower than the energy at the HF geometry (Table V). However, since the MP2 method does not include the effect of single excitations, which has been shown by Almlöf and co-workers[14] to be important, it is likely that the energy will still be underestimated. This fact may be significant if the effect of single excitations in the protonated forms is not as important as it is for ferrocene.

Before considering protonated ferrocene, a smaller system will be investigated which is in some aspects similar to protonated ferrocene and for which there is some experimental data. The metal and ligand protonated forms of Fe—(H_2C=CH_2) (see Figure 1) are known[35,36] to interconvert at room temperature. This suggests that the energy difference must be small. Unlike protonated ferrocene which is low spin, the low-valence complexes are probably high spin. The geometries were calculated at the UHF/BAS2 level, and the energy differences (all quintet states) were calculated up to the PMP4 level of electron correlation (the 'P' indicates that the effects of spin contamination are projected out of the MP4 energy). The results do not differ significantly from an earlier study using the ECPDZ method.[20] Interestingly, electron correlation has only a moderate effect on the preferred site of protonation (Table III), which will be unlike the results obtained for protonated ferrocene. When the metal is protonated for Fe—(H_2C=CH_2), the metal interacts with the π bond of ethylene. In contrast, when the ligand is protonated, the metal interacts to form a σ bond. In both complexes there is one σ interaction. In protonated ferrocene, metal protonation produces a Fe σ bond while ligand protonation does not.

Table III. Energy Separation (kcal/mol) of High-Spin Fe–$C_2H_5^+$/HFe–$C_2H_4^+$ Complexes[a]

	ECPDZ//ECPDZ[b]	BAS2//BAS2
HF	18.5	17.2
PMP2	9.8	9.4
PMP3	10.0	10.0
PMP4		8.5
exptl[c]		0 ± 15

[a] A positive value indicates that Fe–$C_2H_5^+$ is more stable. [b] An 18-electron HW-ECP is used, and a double-ζ basis is used for the 4s, 3d, and 4p valence orbitals. A double-ζ Dunning and Huzinaga basis is used for carbon and hydrogen. Reference 20. [c] References 35 and 36.

Table IV. Calculated Interaction Energy (kcal/mol) of H^+ with Low-Spin Fe and C_2H_4[a]

	FeH^+	$C_2H_5^+$	Δ
HF	−184.2	−175.3	8.9
MP2	−203.4	−162.3	41.1
MP4	−208.6	−164.1	44.5

[a] The calculation for Fe was based on the singlet closed-shell configuration with the d_{z^2} and $d_{x^2-y^2}$ orbitals empty ($4s^23d^6$). The calculation for FeH^+ was for the closed-shell low-spin state. All hydrogens are terminal in the geometry of $C_2H_5^+$.

In order to more accurately predict the effect of electron correlation on the site of protonation, the proton interaction energies of Fe and H_2C=CH_2 were separately calculated with the HF/BAS2 method. Rather than the high-spin ground state of Fe, a closed-shell singlet state of Fe was calculated, since it more closely approximates the electronic environment in ferrocene. The electronic configuration was $4s^23d^6$ with the d_{z^2} and the $d_{x^2-y^2}$ orbitals empty. The calculated electronic state of FeH^+ was the lowest closed-shell singlet state, and the classical form of H_2-CCH_3^+ was calculated (i.e. no bridging hydrogens). The results in Table IV indicate that electron correlation increases the proton interaction energy with Fe significantly while slightly decreasing the proton interaction energy with H_2C=CH_2. The MP2/BAS2 level increases proton binding to Fe relative to H_2C=CH_2 by 32.2 kcal/mol compared to the HF/BAS2 level and 35.6 kcal/mol at the MP4 level. Thus, electron correlation is expected to significantly favor metal protonation in ferrocene.

The optimized geometries of the metal-protonated and ring-protonated ferrocene are given in Figure 2. Total energies are given in Table V, and interaction energies are given in Table VI.

Since an IR study of metal-protonated ferrocene in solution indicates the Cp–Fe–Cp angle is bent,[2] the initial geometry search (within C_{2v} symmetry) was begun with a ring–metal–ring angle of about 140°. At the HF/BAS level, the Cp rings moved back during geometry optimization. However, at the MP2/BAS1, the rings did fold away from the proton with a ring–iron–ring angle of 153.1°. At the HF/BAS2 level, the average metal–carbon distance in metal-protonated ferrocene has actually decreased slightly compared to that in ferrocene (2.156 Å compared to 2.196 Å) while the average metal–carbon distance increased slightly at the MP2/BAS1 level (2.060 Å compared to

(30) Bader, R. F. W. *Atoms in Molecules: A Quantum Theory*; Claredon Press: Oxford, England, 1990.
(31) VECA1M: Cioslowski, J. *Chem. Phys. Lett.*, in press.
(32) PROA1M: Biegler-König, F. W.; Bader, R. F. W.; Tang, T. H. *J. Comput. Chem.* **1982**, *3*, 317.
(33) Cioslowski, J.; Mixon, S. T. *J. Am. Chem. Soc.* **1991**, *113*, 4142.
(34) Cioslowski, J.; Surján, P. R. *THEOCHEM* **1992**, *255*, 9.
(35) Schultz, R. H.; Elkind, J. L.; Armentrout, P. B. *J. Am. Chem. Soc.* **1988**, *110*, 411.
(36) Dearden, D. V.; Beauchamp, J. L.; van Koppen, P. A. M.; Bowers, M. T. *J. Am. Chem. Soc.* **1990**, *112*, 9372.

Table V. Absolute Energies (hartrees) for Ferrocene and Protonated Ferrocene at Various Levels of Theory[a]

	BAS1//BAS2		BAS2//BAS2		BAS3//BAS2	
	HF	MP2	HF	MP2	HF	MP2
$FeCp_2$	-1646.280 16	-1647.324 37	-506.957 34	-508.447 63	-1646.448 17	-1647.962 92
$HFeCp_2^+$	-1646.538 99	-1647.664 00	-507.221 68	-508.785 78	-1646.715 27	-1648.307 02
$FeCpC_5H_6^+$	-1646.628 33	-1647.640 32	-507.306 24	-508.746 82	-1646.798 75	-1648.263 34

	BAS1//MP2/BAS1		BAS3//MP2/BAS1	
	HF	MP2	HF	MP2
$FeCp_2$	-1646.187 49 (58.2)	-1647.376 86 (-32.9)	-1646.362 82 (53.6)	-1648.028 63 (-41.2)
$HFeCp_2^+$	-1646.452 86 (54.0)	-1647.783 92 (-75.2)	-1646.627 27 (55.2)	-1648.430 26 (-77.3)
$FeCpC_5H_6^+$	-1646.469 67 (99.6)	-1647.728 78 (-55.5)	-1646.646 83 (95.3)	-1648.366 45 (-64.7)

[a] In parentheses is the energy change (kcal/mol) at the indicated level when the geometry is optimized at the MP2/BAS1 level rather than the HF/BAS2 level.

Table VI. Calculated Proton Interaction Energies (kcal/mol) for the Metal-Protonated and Ring-Protonated Forms of Ferrocene[a]

	BAS1//BAS2		BAS2//BAS2		BAS3//BAS2		BAS1//MP2/BAS1		BAS3//MP2/BAS1		
	HF	MP2	HF	MP2	HF	MP2	HF	MP2	HF	MP2	Estim PA[b]
$HFeCp_2^+$	-162.4	-213.1	-165.9	-212.2	-167.6	-215.9	-166.5	-255.4	-165.9	-262.0	250.9
$FeCpC_5H_6^+$	-218.5	-198.2	-218.9	-187.7	-220.0	-188.5	-177.1	-220.8	-178.2	-212.0	208.9

[a] Experimental proton affinity of ferrocene is 206–213 kcal/mol.[3,10] [b] Correction for zero-point energy is made by considering only the additional stretch due to the proton. The Fe–H stretch was taken as 1800 cm^{-1}, and the new C–H stretch was taken as 3200 cm^{-1}. A 5/2RT factor was included for heat capacity.

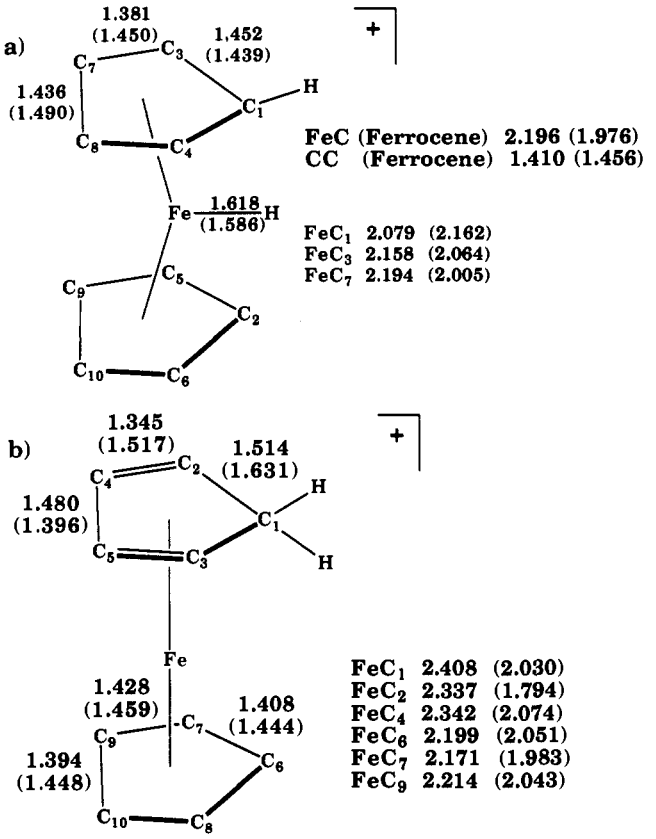

Figure 2. Selected geometric parameters given at the HF/BAS2 level (MP2/BAS1 level in parentheses) for (a) metal-protonated and (b) ring-protonated structures of ferrocene.

1.976 Å). At both levels of geometry optimization, the internal C–C distances in the Cp ring have become unequal (Figure 2), while the average C–C distance remains very close to the value in ferrocene (0.01 Å larger, HF/BAS2; 0.002 Å smaller, MP2/BAS1).

A search was made at the HF/BAS2 level for a metal-protonated structure with the hydrogen interacting agostically[37] with one ring (in C_s symmetry). However, the hydrogen transferred to the ring during the geometry search giving the ring-protonated structure. Since an agostic interaction would stabilize the metal-protonated form, the symmetrical structure (C_{2v} symmetry) can be taken as an upper limit to the stability of this form.

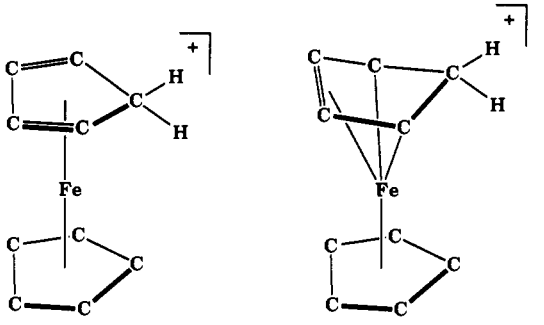

Figure 3. Indication of the change of interaction of the C_5H_6 ligand with iron from the HF/BAS2 level (left) to the MP2/BAS1 level (right). At the HF/BAS2 level, the iron is predicted to interact with two π bonds of cyclopentadiene. At the MP2/BAS1 level, the location of the π bond has migrated and two of the carbons of the C_5H_6 ligand have adopted sp^3 hybridization and interact with the iron in a σ fashion.

Optimizing at the correlated level substantially increased the stability of the metal-protonated form. At the MP2/BAS3 level, the energy using the MP2/BAS1 geometry was 77.3 kcal/mol lower than the energy using the HF/BAS2 geometry, while at the same time the HF/BAS3 energy was 55.2 kcal/mol higher (Table V). The most important contributor to the energy lowering is the reduced metal–ring distance in the MP2/BAS1 geometries.

When the ring-protonated form was optimized at the HF/BAS2 level, the C_5H_6 ligand showed bond lengths only slightly different from those of neutral cyclopentadiene. The protonated ligand has moved 0.16 Å from the iron while the average C–C distance and Fe–C distance of the opposite ring are virtually unchanged relative to those of ferrocene. The most reasonable interpretation of the metal–ligand binding is to consider an Fe(II) ion interacting with a negatively charged Cp ligand and a neutral cyclopentadiene ligand (two π bonds), which gives an electron count of 16 around iron.

(37) Brookhart, M.; Green, M. L. H.; Wong, L.-L. Carbon-Hydrogen Transition Metal Bonds. In *Progress in Inorganic Chemistry*; Lippard, S. J., Ed.; Wiley: New York, 1988; Vol 36, pp 1–124.

Table VII. Calculated Charges for Ferrocene and Protonated Ferrocene at Various Levels of Theory

atom[a]	BAS1//BAS2 HF/Mul	BAS1//BAS2 HF/Bader	BAS2//BAS2 HF/Mul	BAS2//BAS2 MP2/Mul	BAS3/BAS2 HF/Mul	BAS3//MP2/BAS1 HF/Mul
			$FeCp_2$			
Fe	1.16	1.16	0.64	0.29	1.02	0.80
C + H	−0.12	−0.12	−0.06	−0.03	−0.10	−0.08
H	0.21	0.03	0.21	0.19	0.20	0.21
			$HFeCp_2^+$			
H	0.21		0.19	0.13	0.14	0.05
Fe	1.00		0.44	0.06	0.82	0.51
C + H (1, 2)	−0.28		−0.16	−0.03	−0.18	0.18
C + H (3, 4, 5, 6)	0.09		0.11	0.10	0.08	0.00
C + H (7, 8, 9, 10)	0.00		0.06	0.11	0.02	0.02
			$FeCpC_5H_6^+$			
Fe	1.23		0.82	0.43	1.08	0.74
C + H(1)	0.05		0.08	0.08	0.08	0.11
C + H(2,3)	0.01		0.06	0.07	0.05	−0.10
C + H(4,5)	0.06		0.09	0.10	0.08	0.10
C + H(6)	0.04		0.05	0.08	0.01	−0.01
C + H(7,8)	−0.04		−0.01	0.05	−0.05	0.06
C + H(9,10)	−0.20		−0.12	−0.02	−0.17	0.01

[a] Carbon and hydrogen are considered together (C + H). The numbers following refer to equivalent CH units in Figure 2.

On the other hand, the metal–ligand interaction is predicted to be qualitatively different at the MP2/BAS1 level of theory. In the C_5H_6 ligand, the C_4–C_5 distance is short (1.396 Å) while all other C–C distances are greater than 1.5 Å (Figure 3), which would suggest two sp^2 hybridized carbons (C_4, C_5) and three sp^3 hybridized carbons (C_1, C_2, C_3). Another indication of sp^3 hybridization around C_2 and C_3 can be seen by the sum of the angles around each carbon (346.6°), which is substantially smaller than the 360° expected for sp^2 hybridization. Thus, carbon centers C_2 and C_3 form σ bonds with iron, as indicated by much shorter Fe–C distances (1.794 Å). At the same time, the short Fe–C_4/Fe–C_5 distances (2.030 Å) and the C_4–C_5 distance (1.396 Å), which is longer than a normal π bond, indicate a strong olefinic interaction. If one considers iron as Fe(II), the Cp ring as anionic, and the C_5H_6 ring as a neutral ring contributing a π bond and two σ bonds, the electron count remains at 16. In a qualitative sense, there is a preference at the MP2/BAS1 level for two Fe–C σ interactions compared to a C=C double bond plus a iron–olefinic interaction.

At the HF/BAS2 level, the proton interaction energy is much greater for the ring-protonated form compared to the metal-protonated form (−218.9 kcal/mol compared to −165.9 kcal/mol). This result is in direct contrast to the recent work of Jungwirth, Stussi, and Weber[12a] who found the metal-protonated form to be favored at the HF level by 29.1 kcal/mol. However, their model of a proton attached to the ring along the 5-fold axis is not realistic. As anticipated above, the effect of electron correlation is to significantly increase the stability of the metal-protonated form. At the MP2/BAS2 level the interaction energies are −212.2 and −187.7 kcal/mol, with the metal-protonated structure lower in energy than the ring-protonated structure by 24.5 kcal/mol. All-electron calculations, carried out with the BAS1 and BAS3 basis sets, give nearly identical results (Table VI). If geometries are optimized at the MP2/BAS1 level of theory, the results do not qualitatively change. The HF energies still are lower for ring protonation while the MP2 energies are lower for metal protonation. The exothermicity of protonation increases and leads to a protonation energy for ferrocene which is substantially larger than experiment. It can be argued that the MP2/BAS1 level should be able to describe the electronic structure of the protonated forms better than ferrocene, which would lead to an overestimation of the protonation energy. It is known that the effects of single excitations, which are absent in the MP2 treatment, are important for ferrocene.[14] If these effects are associated with metal–Cp interactions, then the description of ferrocene (with two strong Cp interactions) should be poorer than those of either of the two protonated forms. Calculations at the full MP4 level would be helpful in this regard, since the effects of single excitations are included at this level. Unfortunately, the expenses of the full MP4 calculation for molecules of this size are still prohibitive.

Table VIII. Bader Atomic Charges and AOM-Based Covalent Bond Orders for Ferrocene Generated from the HF/BAS1 Basis Set[a]

atom	Q_{Bader}	bond	P_{cov}[b]
Fe	1.16	Fe–C	0.27
C	−0.15	C–C	1.41
H	0.03	C–H	1.00

[a] References 33 and 34. [b] Averaged over the five C–C bond orders. The individual bond orders in the particular localized structure ranged from 1.21 to 1.64.

At the highest level (MP2//BAS3//MP2/BAS1), the interaction of a proton with the metal is −252.0 kcal/mol, which is 40.0 kcal/mol more exothermic than the interaction of a proton with the ring. A very crude estimate can be made of the zero-point and heat-capacity corrections to give a proton affinity. Only the new stretch associated with the added proton will be considered. For the metal-protonated structure, an 1800-cm^{-1} stretch (the experimental[38] Fe–H stretch is 1827 cm^{-1}) will be used, while for the ring-protonated structure a 3200-cm^{-1} C–H stretch will be used. A $^5/_2RT$ correction is used for the heat-capacity correction to 298 K.[39] With these corrections, the estimated proton affinity (PA) is 250.9 kcal/mol, which is larger than the experimental range[10] of 206–210 kcal/mol. The ring-protonated structure has a calculated PA of 208.9 kcal/mol, which is 42.0 kcal/mol smaller than that of the metal site. The PA of the secondary site has been experimentally estimated to be at least 5 or 10 kcal/mol less favorable, which would indicate that the calculated stability of the ring-protonated form is underestimated relative to that of the metal-protonated form.

Population Analysis

An analysis of the charge distribution was made for ferrocene and the protonated forms to understand the changes in electronic structure that take place upon protonation. Mulliken charges are known to be dependent on the basis set and can sometimes give misleading results.[34] This may especially apply to transition metal complexes, since the arbitrary division of overlap between

(38) Armentrout, P. B.; Sunderlin, L. S. Gas-Phase Organometallic Chemistry of Transition Metal Hydrides. In *Transition Metal Hydrides*; Dedieu, A., Ed.; VCH: New York, 1992; pp 1–64.

(39) Eades, R. A.; Scanlon, K.; Ellenbergen, M. R.; Dixon, D. A. *J. Phys. Chem.* **1980**, *84*, 2840.

Table IX. Calculated Mulliken Populations for the Valence Electrons of Fe in Ferrocene and Protonated Ferrocene

	BAS1//BAS2 HF			BAS2//BAS2 HF			BAS2//BAS2 MP2			BAS3//BAS2 HF			BAS3//MP2/BAS1 HF		
	s	p	d	s	p	d	s	p	d	s	p	d	s	p	d
$FeCp_2$	0.26	0.04	6.54	0.40	0.06	6.72	0.43	0.07	7.21	0.38	0.05	6.55	0.47	0.07	6.66
$HFeCp_2^+$	0.29	0.05	6.66	0.44	0.03	7.09	0.47	0.04	7.43	0.44	0.06	6.68	0.56	0.08	6.85
$FeCpC_5H_6^+$	0.28	0.04	6.45	0.40	0.05	6.73	0.40	0.05	7.12	0.40	0.05	6.47	0.54	0.08	6.64

Table X. Calculated Charge Displacement Which Results from Protonating Ferrocene[a]

	BAS1//BAS2 HF		BAS2//BAS2 HF		BAS2//BAS2 MP2		BAS3//BAS2 HF		BAS3//MP2/BAS1 HF	
	Fe	Cp/C_5H_6	Fe	Cp/C_5H_6	Fe	Cp/C_5H_6	Fe	Cp/C_5H_6	Fe	Cp/C_5H_6
$HFeCp_2^+$	0.05	0.95	−0.01	1.01	−0.10	1.10	−0.06	1.06	−0.24	1.24
$FeCpC_5H_6^+$	0.07	0.14/0.77	0.18	0.12/0.70	0.14	0.29/0.57	0.06	0.08/0.85	−0.06	0.53/0.52

[a] The entries represent the differences in the Mulliken charge between ferrocene and the protonated form. The proton is absorbed with Fe in the metal-protonated form and with the Cp ring (i.e. C_5H_6) in the ring-protonated form. The sum of the differences should equal 1, but may not due to round-off error. For the metal-protonated form, both rings are the same. For the ring-protonated form, the change in Mulliken charge in the Cp ring is given first, then that of the C_5H_6 ring (i.e. Cp/C_5H_6).

atomic centers may be inappropriate in this case. However, the Mulliken population analysis may be adequate for studying relative trends.

A method has been described by Bader[30] for determining atomic charges that are less dependent on a chosen basis set. First, critical points in electron density are located; then a surface of zero flux is determined around each attractor (nuclear center), and the volume is integrated. These charges can be rigorously interpreted and have been found to be useful in a variety of contexts.[30] Next, the orbitals are localized by a method described by Cioslowski and the atomic overlap matrix (AOM) is determined,[33,34] the off-diagonal elements of which are the bond orders.

This analysis, which was carried out with the BAS1 basis and HF/BAS2 geometry for ferrocene, is the first application to a metal complexed with a Cp ring. The Mulliken and Bader charges are given in Table VII. Using the BAS1 basis set, both methods give identical results for partitioning charge between the metal and the Cp rings.[40] However, the charge associated with the hydrogens using Bader's method is less positive compared to that from the Mulliken population analysis. The AOM-based covalent bond orders[33,34] reported in Table VIII are for one of several possible localized resonance structures (i.e. different positions of single and double bonds in the Cp ring). The C–C AOM covalent bond orders ranged from 1.21 to 1.64 with an average value of 1.41. In contrast, the C–H (1.00) and Fe–C (0.27) AOM covalent bond orders varied over a much smaller range. The 10 Fe–C bonds produce a total Fe–C bond order of 2.70. The total Fe–C bond order must be underestimated, since it is known that the two Cp groups are bound by a total of 250 kcal/mol[41] and would require an average Fe–C bond of 92 kcal/mol (even greater if promotion energy is considered) while a more reasonable average Fe–C bond energy in an organometallic bond would be less than 60 kcal/mol.[10]

The Mulliken population analysis of the Hartree–Fock wave function was carried out using HF/BAS2 geometries and the BAS1, BAS2, and BAS3 basis sets and using MP2/BAS1 geometries with the BAS3 basis set. In addition, the effect of electron correlation on the population analysis was determined using HF/BAS2 geometries and the wave function calculated at the MP2/BAS2 level. An inspection of the calculated populations for ferrocene and protonated ferrocene indicates that relative to the HF/BAS2 level, electron correlation (MP2/BAS2) reduces the charge on Fe while a more flexible basis set (HF/BAS3) increases the charge on Fe. In fact, the effect of electron correlation (MP2/BAS2) and additional basis set flexibility affect the HF/BAS2 charges nearly equally but in opposite directions. The effect of using MP2/BAS1 rather than HF/BAS2 geometries is to reduce the positive charge on iron by 0.2–0.3 e, which would indicate a greater transfer of electrons from the iron into the empty orbitals on the ligand as the iron–ligand distance is reduced.

The calculated populations of the valence electrons of Fe are tabulated at different levels in Table IX. As found for the charges, the populations at the MP2/BAS2 and HF/BAS3 levels deviate in opposite directions from those at HF/BAS2 level. Electron correlation (MP2/BAS2) increases the d orbital population while a more flexible basis set (HF/BAS3) decreases it. The d orbital populations at the HF/BAS3 level using MP2/BAS1 geometries rather than HF/BAS2 geometries indicate very little change in the d orbital population but a definite increase in the s orbital population. This may be due to electron repulsion as a result of the smaller metal–ligand separation which would favor increased sd_{z^2} hybridization.

Perhaps most noteworthy is the fact that the d orbital population remains approximately the same for ferrocene and both protonated forms. A better insight into the electronic reorganization that takes place upon protonation can be obtained by calculating the charge displacements that occur. In Table X, the transfer of Mulliken charge is calculated between the metal and the two rings. Since one positive charge is added, the sum of the charge differences should equal 1.0 (round-off error may cause a small deviation). For metal protonation, the positive charge is considered part of Fe, while, for ring protonation, it is considered part of one ring. For example, the charge on FeH in the metal-protonated structure (HF/BAS1) is 0.05 e greater than the charge on Fe in ferrocene and the charge (cumulative) on both rings is 0.95 e greater than that in ferrocene. Protonating the metal causes the rings to become more positively charged. From one viewpoint, when the metal is protonated, Fe becomes more electropositive and attracts nearly a full negative charge (1.01 e, HF/BAS2) from the two Cp rings which neutralizes the original +1 charge on the metal. If the ring is protonated, significant charge (0.70 e, HF/BAS2) is retained on the C_5H_6 ring while some charge is pulled from the more distant Cp ring (0.12 e, HF/BAS2) and the metal (0.18 e, HF/BAS2). The charge displacement calculated with MP2/BAS1 geometries is essentially the same. At the HF/BAS3 level and using MP2/BAS1 geometries, metal protonation causes 1.24 e to be pulled from the rings while ring protonation does not change the population on the metal.

(40) A similar result was obtained from a comparison of the Bader and the Mulliken population in hexaaqua- and hexacyano iron complexes. Mandix, K.; Johansen, H. *J. Phys. Chem.* **1992**, *96*, 7261.

(41) Puttemans, J. P.; Smith, G. P.; Golden, D. M. *J. Phys. Chem.* **1990**, *94*, 3227.

The calculations cannot specifically address which site is protonated first, since there may be a difference in the activation barriers for addition to the two sites. Thus, the ring site might protonate more quickly (indeed, there might be no activation barrier) because there is less transfer of charge from the site of protonation (less reorganization required). Metal protonation, on the other hand, requires charge migration from the two rings which might cause the activation barrier to be higher. However, the calculations do indicate that the metal-protonated site is thermodynamically favored.

Conclusions

The two protonation sites in ferrocene have been studied. Protonation on the metal is predicted to be 42.0 kcal/mol more favorable than protonation on the ring. The calculated proton affinity for ferrocene (250.9 kcal/mol) is considerably larger than the experimental range (206–210 kcal/mol), which may be due to the neglect of single excitations in the MP2 treatment which are known to be important in the description of ferrocene. From an analysis of charge, it is concluded that metal protonation causes the transfer of about a full electronic charge from the rings to the metal.

Acknowledgment. I thank the donors of the Petroleum Research Fund, administered by the American Chemical Society, for financial support. Computer time for this study was made available by the Alabama Supercomputer Network and the NSF-supported Pittsburgh Supercomputer Center. I would like to thank Dr. Jerzy Cioslowski for help with the Bader and AOM analysis of ferrocene, Dr. C. E. C. A. Hop for a preprint, and Pavel Jungwirth for helpful discussions.